Inorganic Chemistry

Article

pubs.acs.org/IC

Aggregation-Induced Emissive Copper(I) Complexes for Living Cell Imaging

Xue-Lian Xin,[†] Min Chen,[‡] Yu-bo Ai,[†] Feng-lei Yang,[†] Xiu-Ling Li,*[,†] and Fuyou Li*[,‡]

[†]School of Chemistry and Chemical Engineering & Jiangsu Key Laboratory of Green Synthetic Chemistry for Functional Materials, Jiangsu Normal University, Xuzhou, Jiangsu 221116, China

[‡]Department of Chemistry, Fudan University, Shanghai, 200433, China

Supporting Information

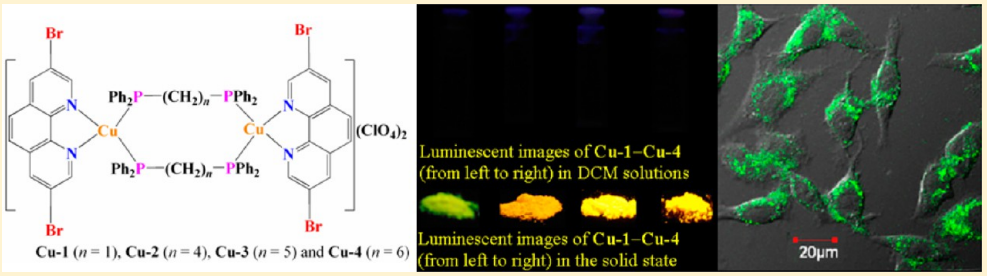

ABSTRACT: Phosphorescent binuclear copper(I) complexes $[Cu_2(BrphenBr)_2(Ph_2P(CH_2)_nPPh_2)_2](ClO_4)_2$ with different conformations are obtained by reaction of $[Cu(NCCH_3)_4]ClO_4$, 3,8-dibromo-1,10-phenanthroline (BrphenBr), and corresponding diphosphine ligands, where n = 1, 4, 5, and 6 in complexes **Cu-1**, **Cu-2**, **Cu-3**, and **Cu-4**, respectively. Complex **Cu-4** exhibits both the eclipsed and the staggered conformations of 18-membered $Cu_2C_{12}P_4$ metallacycles in a 1:1 ratio in the crystal structure. All complexes are very stable to air and moisture in the solid state because of the high level of protection of all the Cu(I) centers, N and P atom centers resulting from the close contact of BrphenBr and diphosphine ligands, and what is more important is that there exist very soft P donors and the chelating effect of aromatic N atoms. The ESI-MS result through changing the collision cell energy from 0 to 20 eV suggests that the corresponding $[Cu_2(Ph_2P(CH_2)_nPPh_2)_2]^{2+}$ cations are the thermodynamically stable species, while $[Cu_2(BrphenBr)_2(Ph_2P(CH_2)_nPPh_2)_2](ClO_4)_2$ are stable products in crystallization kinetics in solutions. All complexes **Cu-1**–**Cu-4** display good aggregation-induced phosphorescence emission (AIPE) behavior in CH_2Cl_2/hexane mixed solvents, which are suggested to arise from restriction of intramolecular rotation. Aggregation-induced emission (AIE) of complexes **Cu-1**–**Cu-4** in PBS/DMSO (99:1, v:v) is used for living HeLa cell imaging successfully with green intracellular emission image.

INTRODUCTION

Heavy-metal complexes that possess d^6, d^8, and d^{10} electron configuration show strong spin–orbit coupling, resulting in efficient intersystem crossing from the singlet excited state to the triplet one and intense phosphorescent emission.[1] Due to the unique characteristics of relative long radiative decay times at the level of microseconds, these phosphorescent heavy-metal complexes as bioimaging probes provide a chance to eliminate autofluorescence from biological sample through time-gated technique. To date, a large of heavy-metal complexes have successfully been developed as photoluminescent probes for bioimaging.[2−19] However, all of the reported phosphorescent complexes for bioimaging are focused on noble metal complexes, including Re(I),[6] Ru(II),[7] Os(II),[8] Ir(III),[9−16] Pt(II),[17,18] and Au(I) complexes,[19] and the relatively high cost of the noble-metal systems will limit their wide application in bioimaging probes. Therefore, it is necessary to design and synthesize noble-metal-free phosphorescent complexes for luminescent bioimaging.

Cu(I) complexes possess d^{10} electronic structure and provide a tunable phosphorescent emission at room temperature and a long luminescence lifetime of several microseconds. To date, a series of Cu(I) complexes has been applied in OLED,[20−30] solar-energy conversion devices,[31,32] and chemosensors.[33−37] Unfortunately, no example of a phosphorescent Cu(I) complex has been reported in application of luminescent bioimaging due to the instability caused by the oxidization and disproportionation of the Cu(I) ion. In the past decade, the study of phosphorescent Cu(I) complexes has mainly focused on Cu(I)–diimine complexes, especially the mixed-ligand Cu(I)–diimine–diphosphine $[Cu(diimine)(PP)]^+$ and $[Cu_2(diimine)_2(PP)_2]^{2+}$ (PP = diphosphine ligand) complexes due to the relatively abundant resource, less expensive noble-metal-free characteristics, controllable electronic and stereochemical characteristics of ligands, and good luminescent performance.[38−53] A recent report showed some Cu(I)–

Received: October 25, 2013
Published: February 21, 2014

Scheme 1. Synthetic Routes to Complexes Cu-1−Cu-4

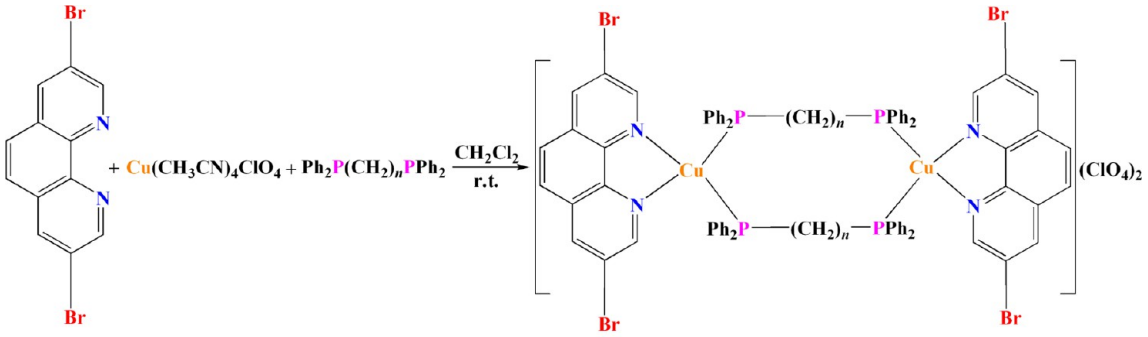

Cu-1 (n = 1), **Cu-2** (n = 4), **Cu-3** (n = 5) and **Cu-4** (n = 6)

diimine−diphosphine complexes can be used as photosensitizers for photocatalytic reduction of protons from water at room temperature.[31] In particular, the binuclear complex $[Cu_2(dmp)_2(dppb)_2](PF_6)_2$ (dmp = 2,9-dimethyl-1,10-phenanthroline, dppb = 1,4-bis(diphenylphosphino)butane) has been proved to be a stronger emitter with a higher quantum yield and a longer lifetime than the corresponding chelating mononuclear $[Cu(dmp)(dppe)]PF_6$ (dppe = 1,2-bis(diphenylphosphino)ethane) and $[Cu(dmp)(dppp)]PF_6$ (dppp = 1,3-bis(diphenylphosphino)propane) complexes (see Figure S1, Supporting Information).[53−55] These observations have attracted our interest to expand the application of $[Cu_2(diimine)_2(PP)_2]^{2+}$ complexes in luminescence bioimaging.

In these present study, four binuclear mixed-ligand Cu(I) complexes $[Cu_2(BrphenBr)_2(Ph_2P(CH_2)_nPPh_2)_2](ClO_4)_2$ (BrphenBr = 3,8-dibromo-1,10-phenanthroline; $Ph_2P(CH_2)_nPPh_2$ = bridging diphosphine ligands, n = 1, 4, 5, or 6, Scheme 1) were designed and synthesized. Interestingly, these four Cu(I) complexes displayed significant aggregation-induced phosphorescence emission (AIPE). Furthermore, the uptake behavior of these Cu(I) complexes with living cells was investigated. This is the first example that Cu(I) complexes with AIPE properties could be used as a phosphorescent probe for luminescence bioimaging.

EXPERIMENTAL SECTION

Materials. The reagents bis(diphenylphosphino)methane (dppm), dppb, 1,5-bis(diphenylphosphino)pentane (dpppen), and 1,6-bis(diphenylphosphino)hexane (dpph) were commercially available and used without further purification. Phosphate-buffered saline (PBS), Fetal Bovine Serum (FBS), and dimethyl sulfoxide (DMSO) were obtained from Acros. BrphenBr and $[Cu(CH_3CN)_4]ClO_4$ were prepared by the published methods.[56,57] All solvents were purified and distilled by suitable procedures before use. All other reagents were of analytical grade and used as received.

Instruments. Infrared (IR) spectra were recorded from KBr pellets using a Bruker Optics TENSOR 27 FT-IR spectrophotometer. UV−vis absorption spectra were determined on a Purkinje General TU-1901 UV−vis spectrophotometer. Elemental analyses (C, H, and N) were carried out on a Perkin-Elmer model 240C elemental analyzer. ^{1}H and ^{31}P NMR spectra were obtained from the solutions in DMSO-d_6 and CD_2Cl_2 using a Bruker-400 spectrometer with Me_4Si as an internal standard and 85% H_3PO_4 as an external standard, respectively. Electrospray ionization mass spectra (ESI-MS) analyses were carried out with a Bruker-micro-TOFQ-MS analyzer using a DCM/methanol mixture for the mobile phase. Steady-state emission spectra were obtained with a Hitachi F4500 fluorescence spectrophotometer. Emission lifetimes were measured on an Edinburgh F900 fluorescence spectrometer under air, and the resulting emission was detected by a thermoelectrically cooled Hamamatsu R3809 photomultiplier tube. The photoluminescence yield in the solid state under air at room temperature is defined as the ratio of the number of photons emitted to the number of photons absorbed by the system and was measured under air on an Edinburgh analytical instrument FLS920 with an integrating sphere established by Wrighton et al.[58]

Cell Culture. The HeLa (Human epithelial cervical cancer cell line) was provided by the Institute of Biochemistry and Cell Biology, Chinese Academy of Sciences. The HeLa cells were grown in RPMI 1640 (Roswell Park Memorial Institute's Medium) supplemented with 10% FBS at 37 °C and 5% CO_2. Cells were plated on 18 mm glass coverslips and allowed to adhere for 24 h.

Confocal Luminescence Imaging. The 1 mM stock solutions of **Cu-1−Cu-4** were prepared in DMSO and then diluted to 10 μM with PBS. Incubation of HeLa cells with 10 μM complexes **Cu-1−Cu-4** in PBS/DMSO (99:1, v/v, pH = 7.4) for 15 min was used for imaging experiments. Confocal luminescence imaging of cells was performed with an OLYMPUS FV1000 confocal fluorescence microscope equipped with a 60× oil-immersion objective lens, excitation at 405 nm was carried out with a semiconductor laser, and the emission was collected at 520 ± 20 nm.

Synthesis of Complexes. All reactions were carried out under anhydrous and anaerobic conditions using standard Schlenk techniques under an atmosphere of dry argon at room temperature.

$[Cu_2(BrphenBr)_2(\mu\text{-dppm})_2](ClO_4)_2{\cdot}2CH_2Cl_2$ (***Cu-1*·2CH_2Cl_2**). $[Cu(CH_3CN)_4]ClO_4$ (32.6 mg, 0.100 mmol) was added to a degassed DCM solution (about 10 mL) of BrphenBr (33.6 mg, 0.100 mmol) and dppm (39.2 mg, 98%, 0.100 mmol). A pale yellow solution was obtained quickly and then stirred for 5 h at room temperature. After filtration, layering n-hexane onto the DCM solution produced the product as pale yellow crystals in 61.7% yield (59.6 mg). Anal. Calcd for $C_{76}H_{60}Br_4Cl_6Cu_2N_4O_8P_4$: C, 47.04; H, 3.12; N, 2.89. Found: C, 47.40; H, 3.24; N, 2.95. ESI-MS (m/z): 831.15 $[Cu(dppm)_2]^+$ (calcd 831.17); 784.933 $[Cu_2(BrphenBr)_2(\mu\text{-dppm})_2]^{2+}/2$ (calcd 784.937); 738.7050 $[Cu(BrphenBr)_2]^+$ (calcd 738.7047); 616.990 $[Cu_2(BrphenBr)(\mu\text{-dppm})_2]^{2+}/2$ (calcd 616.993); 593.878 $[Cu_2(BrphenBr)_2(\mu\text{-dppm})]^{2+}/2$ (calcd 593.877); 447.042 $[Cu_2(\mu\text{-dppm})_2]^{2+}/2$ (calcd 447.049). ^{1}H NMR (400 MHz, DMSO-d_6, δ, ppm): 8.963 (s, 4H, Br*phen*Br), 8.615 (s, 4H, Br*phen*Br), 7.952 (s, 4H, Br*phen*Br), 7.139−6.945 (m, 40H, PPh_2), 4.235 (br, 4H, PCH_2P). ^{31}P NMR {^{1}H NMR} (400 MHz, DMSO-d_6, δ, ppm): −5.265, −10.027. ^{1}H NMR (400 MHz, CD_2Cl_2, δ, ppm): 8.636 (s, 4H, Br*phen*Br), 8.598 (s, 4H, Br*phen*Br), 7.930 (s, 4H, Br*phen*Br), 7.173−6.992 (m, 40H, PPh_2), 4.068 (m, 4H, PCH_2P). ^{31}P NMR {^{1}H NMR} (400 MHz, CD_2Cl_2, δ, ppm): −7.992, −14.544. IR spectrum (KBr, cm^{-1}): 1096vs (ClO_4^-).

$[Cu_2(BrphenBr)_2(\mu\text{-dppb})_2](ClO_4)_2{\cdot}4CH_2Cl_2$ (***Cu-2*·4CH_2Cl_2**). This complex was prepared by the same procedure as that of **Cu-1** except for the use of dppb instead of dppm. Yield: 80.2%. Anal. Calcd for $C_{84}H_{76}Br_4Cl_{10}Cu_2N_4O_8P_4$: C, 45.97; H, 3.49; N, 2.55. Found: C, 46.32; H, 3.70; N, 2.53. ESI-MS (m/z): 827.981 $[Cu_2(BrphenBr)_2(\mu\text{-dppb})_2]^{2+}/2$ (calcd 827.984); 489.090 $[Cu_2(\mu\text{-dppb})_2]^{2+}/2$ (calcd 489.096). ^{1}H NMR (400 MHz, DMSO-d_6, δ, ppm): 9.086 (s, 4H,

dx.doi.org/10.1021/ic402685u | Inorg. Chem. 2014, 53, 2922−2931

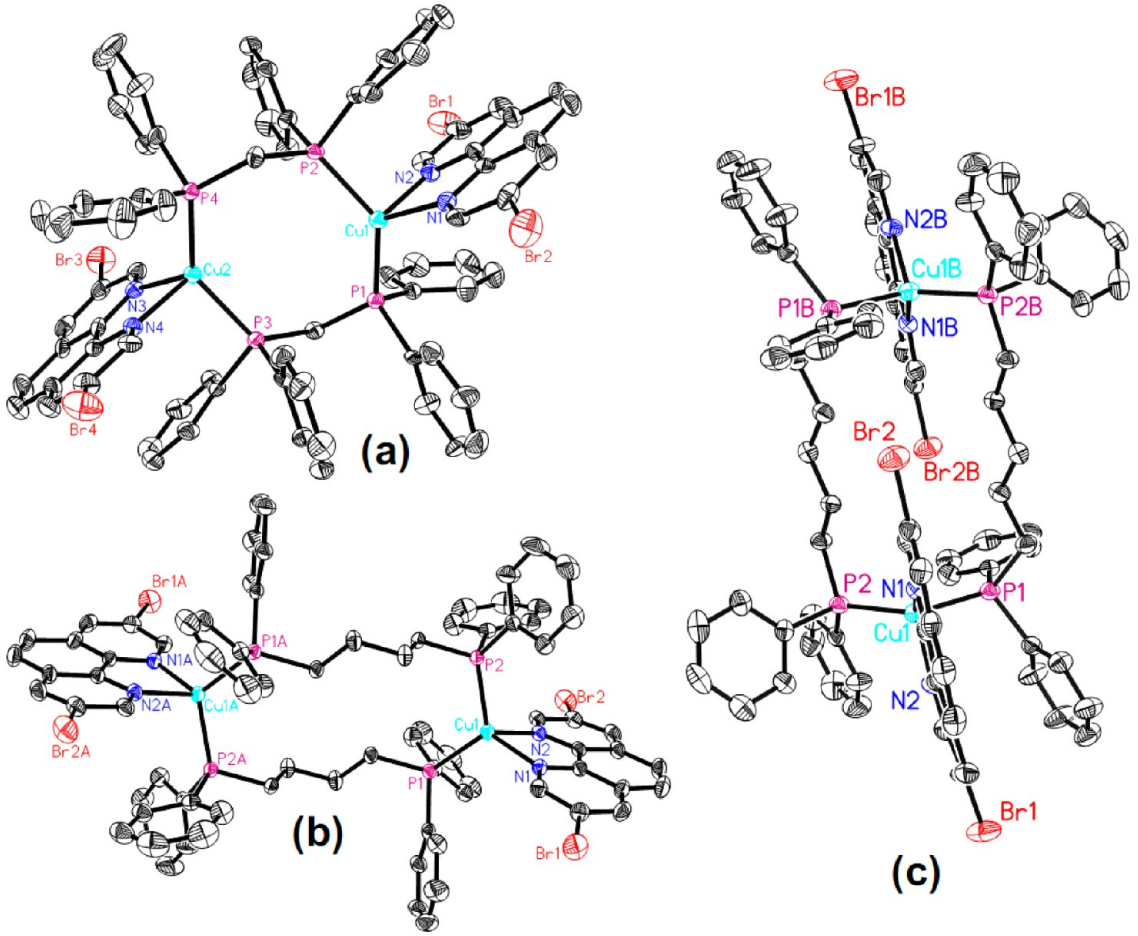

Figure 1. ORTEP drawings of the cation structures of complexes **Cu-1** (a), **Cu-2** (b), and **Cu-3** (c) with atom-labeling scheme, showing 30% thermal ellipsoids. Hydrogen atoms are omitted for clarity (symmetry codes for A $-x + 1, -y + 2, -z + 2$; B $-x, -y + 1, -z + 1$).

Br*phen*Br), 8.787 (s, 4H, Br*phen*Br), 8.163 (s, 4H, Br*phen*Br), 7.362–7.048 (m, 40H, PPh_2), 2.777 (br, 8H, PCH_2CH$_2$CH$_2$CH_2P); 2.005 (br, 8H, PCH$_2$CH_2CH_2CH$_2$P). ^{31}P NMR {^{1}H NMR} (400 MHz, DMSO-d_6, δ, ppm): −2.471, −5.555. ^{1}H NMR (400 MHz, CD_2Cl_2, δ, ppm): 8.675 (s, 4H, Br*phen*Br), 8.323 (s, 4H, Br*phen*Br), 8.045 (s, 4H, Br*phen*Br), 7.446–7.101 (m, 40H, PPh_2), 2.654 (br, 8H, PCH_2CH$_2$CH$_2$CH_2P), 2.232 (br, 8H, PCH$_2$CH_2CH_2CH$_2$P). ^{31}P NMR {^{1}H NMR} (400 MHz, CD_2Cl_2, δ, ppm): −1.608, −5.685. IR spectrum (KBr, cm^{-1}): 1094vs (ClO_4^-).

[Cu_2(BrphenBr)$_2$(μ-dpppen)$_2$](ClO_4)$_2$·4CH_2Cl_2 (**Cu-3**·4CH_2Cl_2). This complex was prepared by the same procedure as that of **Cu-1** except for the use of dpppen instead of dppm. Yield: 57.3%. Anal. Calcd for $C_{86}H_{80}Br_4Cl_{10}Cu_2N_4O_8P_4$: C, 46.47; H, 3.63; N, 2.52. Found: C, 46.87; H, 3.88; N, 2.58. ESI-MS (m/z): 841.008 [Cu_2(BrphenBr)$_2$(μ-dpppen)$_2$]$^{2+}$/2 (calcd 840.999); 503.07 [Cu_2(μ-dpppen)$_2$]$^{2+}$/2 (calcd 503.11). ^{1}H NMR (400 MHz, DMSO-d_6, δ, ppm): 9.028 (s, 4H, Br*phen*Br), 8.668 (s, 4H, Br*phen*Br), 8.065 (s, 4H, Br*phen*Br), 7.340–7.134 (m, 40H, PPh_2), 2.612 (br, 8H, PCH_2CH$_2$CH$_2$CH$_2$CH_2P), 2.205 (br, 4H, PCH$_2$CH$_2$CH_2CH$_2$CH$_2$P), 1.773 (br, 8H, PCH$_2$CH_2CH$_2$CH_2CH$_2$P). ^{31}P NMR {^{1}H NMR} (400 MHz, DMSO-d_6, δ, ppm): −2.986, −7.079. ^{1}H NMR (400 MHz, CD_2Cl_2, δ, ppm): 8.628 (s, 4H, Br*phen*Br), 8.494 (s, 4H, Br*phen*Br), 7.928 (s, 4H, Br*phen*Br), 7.390–7.120 (m, 40H, PPh_2), 2.534–2.418 (m, 12H, PCH_2CH$_2$CH_2CH$_2$CH_2P), 1.879 (br, 8H, PCH$_2$CH_2CH$_2$CH_2CH$_2$P). ^{31}P NMR {^{1}H NMR} (400 MHz, CD_2Cl_2, δ, ppm): −8.316. IR spectrum (KBr, cm^{-1}): 1091vs (ClO_4^-).

[Cu_2(BrphenBr)$_2$(μ-dpph)$_2$](ClO_4)$_2$·4CH_2Cl_2 (**Cu-4**·4CH_2Cl_2). This complex was prepared by the same procedure as that of **Cu-1** except for the use of dpph instead of dppm. Yield: 45.0%. Anal. Calcd for $C_{88}H_{84}Br_4Cl_{10}Cu_2N_4O_8P_4$: C, 46.96; H, 3.76; N, 2.49. Found: C, 47.36; H, 3.93; N, 2.56. ESI-MS (m/z): 856.05 [Cu_2(BrphenBr)$_2$(μ-dpph)$_2$]$^{2+}$/2 (calcd 856.02); 517.18 [Cu_2(μ-dpph)$_2$]$^{2+}$/2 (calcd 517.13). ^{31}P NMR {^{1}H NMR} (400 MHz, DMSO-d_6, δ, ppm): −2.745, −3.307, −3.921, −10.393. ^{1}H NMR (400 MHz, CD_2Cl_2, δ, ppm) for the isomer with staggered conformation: 8.649 (d, J = 1.6 Hz, 4H, Br*phen*Br), 8.520 (s, 4H, Br*phen*Br), 7.963 (s, 4H, Br*phen*Br), 7.365–7.027 (m, 40H, PPh_2), 2.579 (m, 16H, PCH_2CH$_2$CH$_2$CH$_2$CH_2CH$_2$P), 1.884 (m, 8H, PCH$_2$CH$_2$CH_2CH_2CH$_2$CH$_2$P). ^{1}H NMR (400 MHz, CD_2Cl_2, δ, ppm) for the isomer with eclipsed conformation: 8.602 (d, J = 1.6 Hz, 4H, Br*phen*Br), 8.506 (s, 4H, Br*phen*Br), 7.862 (s, 4H, Br*phen*Br), 7.365–7.027 (m, 40H, PPh_2), 2.044 (m, 8H, PCH_2CH$_2$CH$_2$CH$_2$CH_2CH$_2$P); 1.700 (m, 16H, PCH$_2$CH_2CH_2CH_2CH_2CH$_2$P). ^{31}P NMR {^{1}H NMR} (400 MHz, CD_2Cl_2, δ, ppm): −2.579, −3.602, −10.733. IR spectrum (KBr, cm^{-1}): 1097vs (ClO_4^-).

RESULTS AND DISCUSSION

Synthesis of the Cu(I) Complexes. Binuclear complexes **Cu-1**–**Cu-4** crystallized as dichloromethane solvates in moderate yields (**Cu-2** ≫ **Cu-1** > **Cu-3** > **Cu-4**) by reaction of equimolar Cu(CH$_3$CN)$_4$ClO$_4$, chelating BrphenBr, and bridging diphosphine ligands with different length of spacers in dichloromethane (DCM) solution. No obvious color change was observed for solid complexes after they were kept in water for a month, indicating that all complexes are very stable to air and moisture in the solid state.

Crystallographic Studies. Single crystals for **Cu-1**·2CH_2Cl_2, **Cu-2**·4CH_2Cl_2, and **Cu-4**·4CH_2Cl_2 were obtained

dx.doi.org/10.1021/ic402685u | *Inorg. Chem.* 2014, 53, 2922–2931

by layering *n*-hexane onto the corresponding DCM solutions. The quality of crystals of **Cu-3**·4CH_2Cl_2 obtained from hexane/DCM is very poor for single-crystal X-ray determination. **Cu-3**·2CH_3CN was obtained by layering diethyl ether onto the corresponding acetonitrile solution in the absence of light. They were measured on Bruker Smart APEX II diffractometers by the ω scan technique at room temperature with graphite-monochromated Mo Kα radiation (λ = 0.71073 Å). The CrystalClear software package 2005[59] and Bruker SAINT and the CrystalClear software package 2007 were used for data reduction and empirical absorption correction, respectively.[60,61] Structures were solved by direct method. Heavy atoms were located from the E-map, and the remaining non-hydrogen atoms were found in subsequent Fourier maps. Non-hydrogen atoms were refined anisotropically, whereas hydrogen atoms were generated geometrically with isotropic thermal parameters. Structures were refined on F^2 by full-matrix least-squares methods using the SHELXTL-97 program package.[62]

The corresponding crystallographic data and select refinement details of complexes **Cu-1**−**Cu-4** are presented in Table S1 (see Supporting Information). Selected bond lengths and angles are listed in Table S2 (see Supporting Information). ORTEP drawings of the cations for **Cu-1**−**Cu-4** are depicted in Figures 1 and 2. All complexes exhibit binuclear structures,

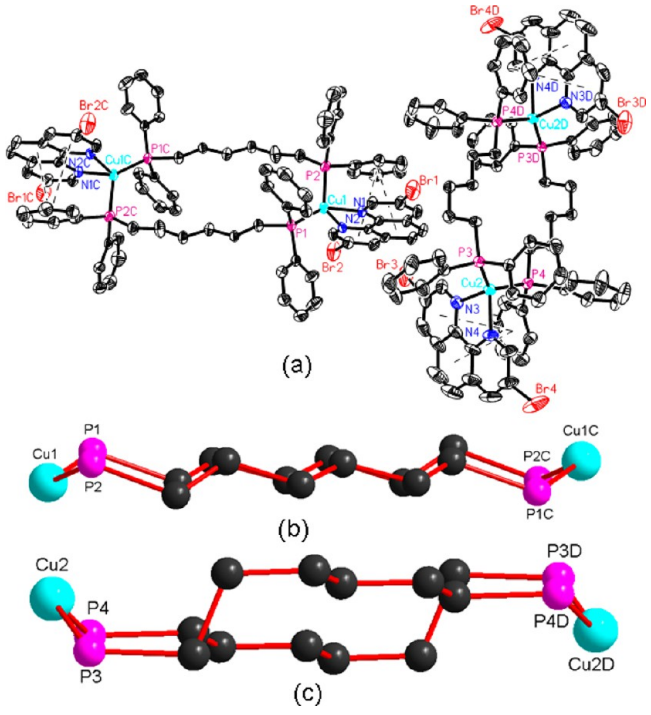

Figure 2. (a) ORTEP drawings of two asymmetric cations of complex **Cu-4** with atom-labeling scheme, showing 30% thermal ellipsoids. Hydrogen atoms are omitted for clarity (symmetry codes for C $-x+1, -y+1, -z+2$; D $-x+2, -y+2, -z+1$); (b) 18-membered $Cu_2C_{12}P_4$ ring with eclipsed conformation; (d) 18-membered $Cu_2C_{12}P_4$ ring with staggered conformation.

which are similar to those of $[Cu_2(BrbpyBr)_2(Ph_2P(CH_2)_nPPh_2)_2](ClO_4)_2$ (n = 1, 4, 5, and 6) and $[Cu_2(dmp)_2(dppb)_2](PF_6)_2$ complexes reported by us and others.[38,53] The two $[Cu(BrphenBr)]^+$ units are bridged by two diphosphine ligands forming 8-membered $Cu_2C_2P_4$, 14-membered $Cu_2C_8P_4$, 16-membered $Cu_2C_{10}P_4$, and 18-membered $Cu_2C_{12}P_4$ metallacycles in **Cu-1**, **Cu-2**, **Cu-3**, and **Cu-4**, respectively. It is interesting to note that these metallacycles adopt different conformations, and those metallacycles of **Cu-1**−**Cu-3** in the crystals adopt staggered conformations (see Figure S2, Supporting Information), but 18-membered $Cu_2C_{12}P_4$ metallacycles of **Cu-4** adopt both eclipsed and staggered conformations (see Figure 2). The cocrystal product of **Cu-4** contains both conformations of a ratio 1:1.

All Cu(I) centers adopt distorted tetrahedral coordinated geometries completed by two N atoms from chelating BrphenBr ligands and two P atoms from bridging diphosphine ligands. The distortion is mainly induced by the rigid BrphenBr ligand, which restricts the N−Cu−N bite angles to 79.0(3)° for **Cu-1**, 79.7(1)° for **Cu-2**, 79.4(3)° for **Cu-3**, and 80.3(2)° and 79.9(2)° for **Cu-4**. The corresponding P−Cu−P angles are 136.2(1)° for **Cu-1**, 118.3(1)° for **Cu-2**, 125.4(1)° for **Cu-3**, and 127.3(1)° and 126.3(1)° for **Cu-4**, showing much variation to each other, but they are very similar to those in binuclear $[Cu_2(BrbpyBr)_2(Ph_2P(CH_2)_nPPh_2)_2](ClO_4)_2$ complexes[38] and much larger than 91.0(1)° in mononuclear [Cu(BrphenBr)(bdpp)]ClO_4 complex.[39] Such similarity or difference depends on whether the diphosphine ligand adopts a bridging mode or a chelating mode. The dihedral angles between the P−Cu−P and the N−Cu−N planes shown in Figure S3 (see Supporting Information) are 89.0(2)° for **Cu-1**, 88.4(1)° for **Cu-2**, 86.0(2)° for **Cu-3**, and 87.2(2)° and 88.3(1)° for **Cu-4**, which are a little smaller than 89.6° in mononuclear complex [Cu(BrphenBr)(bdpp)]ClO_4[39] and similar to 86.2(1)−88.6(2)° in binuclear $[Cu_2(BrbpyBr)_2(Ph_2P(CH_2)_nPPh_2)_2](ClO_4)_2$ complexes.[2] Both the larger P−Cu−P angles and the smaller dihedral angles imply that the PPh_2 groups in these binuclear complexes are sterically much closer to the BrphenBr ligands than those in the mononuclear complex [Cu(BrphenBr)(bdpp)]ClO_4,[38] and this can be seen from Figures 1 and 2 and Figure S4 (see Supporting Information, the space fillings of cations of complexes **Cu-1**−**Cu-4**). As shown in Figure S4, Supporting Information, all copper(I) centers, together with coordinated N and P atoms, are effectively protected by the phenyl rings, methylene groups of diphosphine ligands, and bromine atoms of BrphenBr in complexes **Cu-1**−**Cu-4**, implying that complexes **Cu-1**−**Cu-4** are very stable to air and moisture in the solid state. More importantly, the soft P donors and chelating effect of aromatic N atoms play a main role for the stability of these complexes.

It is worth noting that the orientations of BrphenBr ligands relative to diphosphine ligands are much different in different complexes. This can be concluded from the intersection angles between the line of two Br atoms in the same BrphenBr ligand and the line of two P atoms in the same diphosphine ligand within a complex (see Figure S5, Supporting Information). The intersection angles are 80.5° between line Br1···Br2 and line P1···P3, 79.0° between line Br1···Br2 and line P2···P4, 80.4° between line Br3···Br4 and line P1···P3, and 78.9° between line Br3···Br4 and line P2···P4 in complex **Cu-1**, 108.1° between line Br1···Br2 and line P1···P2A in complex **Cu-2**, 12.4° between line Br1···Br2 and line P1···P2B in complex **Cu-3**, 63.6° between line Br1···Br2 and line P1···P2C and 138.6° between line Br3···Br4 and line P3···P4D in complex **Cu-4** (symmetry codes for A $-x+1, -y+2, -z+2$; B $-x, -y+1, -z+1$; C $-x+1, -y+1, -z+2$; D $-x+2, -y+2, -z+1$). Complex **Cu-3** shows the smallest intersection angle, indicating that the BrphenBr ligands are almost in parallel with $P(CH_2)_5P$ units in complex **Cu-3**. In complexes **Cu-1** and **Cu-2**, the two kinds of ligands are almost perpendicular to each other. As

dx.doi.org/10.1021/ic402685u | *Inorg. Chem.* 2014, 53, 2922−2931

shown in Figure S4, Supporting Information, the almost parallel arrangement of two kinds of ligands in complex **Cu-3** provides better protection for the Cu(I) centers than other complexes in the solid state. Complex **Cu-3** shows possible double intermolecular $\pi\cdots\pi$ interactions between BrphenBr ligands with the distances of the two ring centroids being 3.672 Å (see Figure S6 and Table S3, Supporting Information), which can only be used as a reference because of the poor crystal quality of **Cu-3**. Complex **Cu-4** show obvious intramolecular $\pi\cdots\pi$ interactions between BrphenBr ligand and dpph with the distances of the two ring centroids falling in the range of 3.662−3.727 Å (see Figure 2 and Table S3, Supporting Information).[3] The Cu−N and Cu−P bond lengths are in the ranges 2.082(3)−2.160(7) and 2.216(2)−2.283(2) Å, respectively, which are similar to those observed in other Cu(I)−diimine−phosphine complexes.[31,32,35,36,38−40,42−53]

^{1}H NMR and ^{31}P NMR Spectra. ^{1}H NMR spectra of BrphenBr and ^{1}H and ^{31}P NMR spectra of **Cu-1**−**Cu-4** recrystallized samples in both DMSO-d_6 and CD_2Cl_2 are provided in the Supporting Information, Figures S7−S24, and data have been listed in the Experimental Section. Because the recrystallized samples of **Cu-2** and **Cu-3**, especially **Cu-3**, are less soluble in CD_2Cl_2 than those of **Cu-2** and **Cu-4**, the ^{1}H NMR and ^{31}P NMR spectra of **Cu-2** and **Cu-3** in CD_2Cl_2 are collected with 64 and 4096 repeated scanning times, respectively, twice as many as those used for **Cu-1** and **Cu-4**. ^{1}H NMR data of **Cu-4** in DMSO-d_6 are not assigned in this article because the ^{1}H NMR solvent residual peak of DMSO at about 2.50 pm overlaps part of the methylene signals. ^{31}P NMR spectra of **Cu-1**, **Cu-2**, and **Cu-3** exhibit a weak signal and a strong one with ratios at 3:1000, 5:100, and 17:100 in DMSO-d_6, while those of **Cu-1** and **Cu-2** in CD_2Cl_2 are 1:100 and 5:100. The ^{31}P NMR signal of **Cu-3** in CD_2Cl_2 is very weak, and only the strong signal can be observed. The integral ratios of the weak signal relative to the strong one increase with increasing methylene length of the diphosphine ligands and do not show an obvious increasing tendency when the coordinating solvent DMSO-d_6 is used instead of the noncoordinating solvent CD_2Cl_2, especially for **Cu-1** and **Cu-2**, so the weak signals are suggested from the different conformations, not from the species based on the dissociation. In addition, no free ^{1}H NMR BrphenBr signals were found, further indicating no obvious dissociation occurred in the experimental conditions. For **Cu-4**, three and four sets of ^{31}P NMR signals are observed in CD_2Cl_2 and DMSO-d_6, respectively. It is difficult to give an exact integral ratio for ^{31}P NMR spectra of **Cu-4** since some of them overlap with each other. The two main sets of NMR signals observed for both ^{1}H NMR and ^{31}P NMR spectra are suggested to arise from two main different conformations (eclipsed conformation and staggered conformation) discussed in the crystallographic part, and the relatively weak signals are suggested to arise from other conformations except for the two main species. On the basis on the above results, the discussion about conformations in the crystallographic part, and the comparison of the P NMR spectra among the series, ^{31}P NMR signals with δ at −5.265, −5.555, −7.079, and −10.393 ppm in DMSO-d_6 and −7.992, −5.685, −8.316, and −10.733 ppm in CD_2Cl_2 for **Cu-1**, **Cu-2**, **Cu-3**, and **Cu-4**, respectively, are suggested from the staggered conformation, while signals with δ at −10.027, −2.471, −2.986, and −2.745 ppm for **Cu-1**, **Cu-2**, **Cu-3**, and **Cu-4** in DMSO-d_6 and −14.544, −1.608, and −2.579 ppm for **Cu-1**, **Cu-2**, and **Cu-4** in CD_2Cl_2 are suggested from the eclipsed conformation.

ESI-MS and Ionization Behavior under Different Collision Cell Energy. As a part of the study of the chemistry of Cu(I)−diimine−diphosphine systems, some attention must be given to the systematic treatment of topics related to the composition and stability of complexes in solutions. Here, we devote our attention to the ionization behavior of complexes **Cu-1**−**Cu-4** under ESI-MS conditions first. In our previous work, $[Cu_2(BrbpyBr)_2(Ph_2P(CH_2)_nPPh_2)_2](ClO_4)_2$ (n = 1, 4, 5, 6) complexes have been suggested to be kinetically stable products in DCM solutions according to the crystalline products and MS results;[38] however, when more rigid BrphenBr instead of BrbpyBr is used, what will happen? Understanding the corresponding thermodynamic behavior will be very helpful for rational molecular design and practical application of such complexes. Thus, here, the ionizing behavior of complexes **Cu-1**−**Cu-4** in DCM solutions was studied by ESI-MS through changing the collision cell energy (CCE) successively from 0 to 20 eV, increasing each time by steps of 5 eV, from soft ionization to hard ionization (see Figure 3 and Figures S25−S27, Supporting Information). When

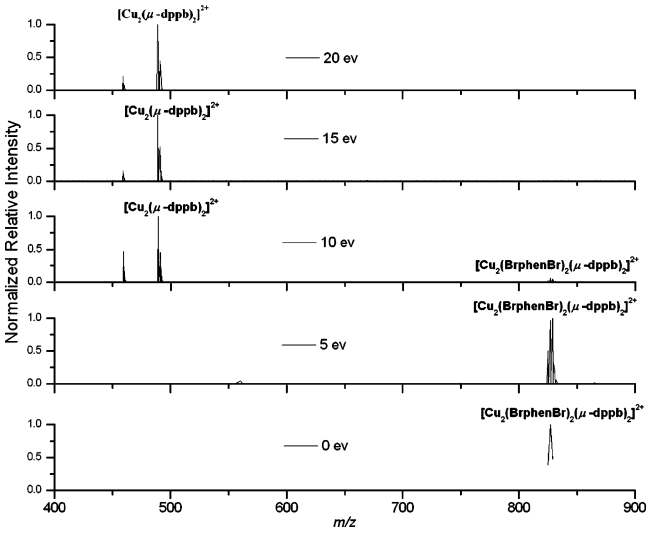

Figure 3. ESI-MS results of complex **Cu-2** with collision cell energy changing from 0 to 20 eV.

CCE is 0 eV, $[Cu_2(BrphenBr)_2(Ph_2P(CH_2)_nPPh_2)_2]^{2+}$ ions are mainly positive species, though the ionization efficiency and absolute abundance of ion current are low. When CCE increases, $[Cu_2(BrphenBr)_2(Ph_2P(CH_2)_nPPh_2)_2]^{2+}/2$ peaks reduce in relative intensity while $[Cu_2(Ph_2P(CH_2)_nPPh_2)_2]^{2+}/2$ peaks increase rapidly. These $[Cu_2(Ph_2P(CH_2)_nPPh_2)_2]^{2+}$ fragment ions are very stable even at CCE of 20 eV, confirming that the binding stability between Cu(I) and BrphenBr is much smaller than that between Cu(I) and diphosphine ligands, which agrees well with the HSAB rules.[63] Analyzing the ESI-MS results at 0 and 5 eV, it is suggested that the degree of ionization for $[Cu_2(BrphenBr)_2(Ph_2P(CH_2)_nPPh_2)_2]^{2+}$ cations exhibits the following order: $[Cu_2(BrphenBr)_2(\mu\text{-dpph})_2]^{2+}$ > $[Cu_2(BrphenBr)_2(\mu\text{-dpppen})_2]^{2+}$ > $[Cu_2(BrphenBr)_2(\mu\text{-dppm})_2]^{2+}$ ≫ $[Cu_2(BrphenBr)_2(dppb)_2]^{2+}$. Thus, the stability order is suggested to be $[Cu_2(BrphenBr)_2(\mu\text{-dppb})_2]^{2+}$ ≫ $[Cu_2(BrphenBr)_2(\mu\text{-dppm})_2]^{2+}$ > $[Cu_2(BrphenBr)_2(\mu\text{-dpppen})_2]^{2+}$ > $[Cu_2(BrphenBr)_2(\mu\text{-dpph})_2]^{2+}$, corresponding

dx.doi.org/10.1021/ic402685u | Inorg. Chem. 2014, 53, 2922−2931

Table 1. Photophysical Data of Cu-1−Cu-4 at Room Temperature

compd	λ_{abs}/nm (ε/M^{-1} cm^{-1}) (CH_2Cl_2)	λ_{em}/nm (CH_2Cl_2)	λ_{em}/nm (solid)	$\tau_{em}{}^{a}$/μs (solid)	$\Phi_{em}{}^{b}$ (solid)
Cu-1	241 (110 000), 281 (64 780), 315 (27 790), 377 (4790)	418, 571	543	4.78	
Cu-2	229 (108 000), 242 (119 300), 284 (82 790), 318 (33 420), 345 (7070), 422 (8200)	418, 483	565	3.96	
Cu-3	229 (88 100), 242 (116 800), 283 (75 490), 318 (30 020), 344 (7310), 406 (7130)	481, 561	559	9.26	0.174
Cu-4	229 (87 020), 243 (114 600), 270 (72 570), 284 (67 610), 342 (7760), 391 (6990)	472, 566	566	2.51	

[a]Solid-state emission lifetimes and. [b]Solid-state quantum yields were determined under air.

to the order of the yield **Cu-2** ≫ **Cu-1** > **Cu-3** > **Cu-4**. Considering the above results and crystallized products in solutions, complexes **Cu-1**−**Cu-4** are suggested to be only kinetically stable products, not thermally stable products in DCM solutions.

Photophysical Properties. *Absorption Spectra.* UV−vis absorption data of complexes **Cu-1**−**Cu-4** in DCM solutions with concentration of 2.5×10^{-5} mol·L^{-1} at room temperature are summarized in Table 1, while the corresponding electronic absorption spectra are depicted in Figure 4. Compared with the

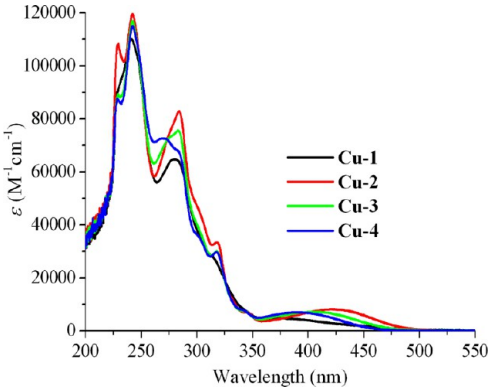

Figure 4. UV−vis absorption spectra of **Cu-1**−**Cu-4** in DCM at room temperature.

absorptions of diphosphine and BrphenBr ligands along with the reported $[Cu(diimine)(PP)]^+$ and $[Cu_2(diimine)_2(PP)_2]^{2+}$ analogs,[38,39,49,50,53,64,65] the intense bands with wavelengths shorter than ca. 350 nm are assigned to ligand-centered $\pi \rightarrow \pi^*$ transitions of coordinated diphosphine ligands and BrphenBr ligands, while the new, weak, broad bands with wavelengths longer than ca. 350 nm are assigned to metal-to-ligand charge transfer ($d\pi(Cu) \rightarrow \pi^*$(BrphenBr)) (MLCT) transitions. The absorption maximum wavelengths of MLCT transitions in complexes **Cu-1**, **Cu-2**, **Cu-3**, and **Cu-4** are 377, 422, 406, and 391 nm, respectively.

Dissociation Behavior in DCM Solution. In order to further explore the composition, dissociation, and stability of complexes in solutions, here, the dissociation behavior of complexes **Cu-1**−**Cu-4** when they are diluted in DCM solutions is studied. Plots of absorption spectra from 2.5×10^{-5} to 4.0×10^{-7} mol·L^{-1} are depicted in Figure S28, Supporting Information. The normalized absorption spectra of complex **Cu-2** at four different concentrations almost overlap with each other, and its MLCT absorption remains very stable. It can be observed that complexes **Cu-2**−**Cu-4** dissociate little with concentrations in the range from 2.0×10^{-6} to 2.5×10^{-5} mol·L^{-1}. For complex **Cu-1**, the MLCT absorption is not obvious even at 2.0×10^{-6} mol·L^{-1}, indicating that dissociation of $[Cu_2(BrphenBr)_2(\mu\text{-dppm})_2]^{2+}$ increases rapidly with dilution. When the solutions are further diluted to 4.0×10^{-7} mol·L^{-1}, the dissociation increases rapidly, and this is particularly evident for complexes **Cu-1** and **Cu-4**, because their MLCT absorption disappears completely. It can be concluded that complexes **Cu-2**−**Cu-4** in solutions in the range from 2.0×10^{-6} to 2.5×10^{-5} mol·L^{-1} agree well with their corresponding solid state, but for complex **Cu-1** there likely exists a ligation on−off equilibrium in diluted solution. The solid state may be different from what is present in diluted solution in composition due to the dissociation. On the basis of the above discussion, it can be concluded that the degree of dissociation exhibits the following order: $[Cu_2(BrphenBr)_2(dppm)_2]^{2+}$ > $[Cu_2(BrphenBr)_2(dpph)_2]^{2+}$ > $[Cu_2(BrphenBr)_2(dpppen)_2]^{2+}$ > $[Cu_2(BrphenBr)_2(dppb)_2]^{2+}$. This indicates the following stability order of composition: **Cu-2** > **Cu-3** > **Cu-4** > **Cu-1**, a little different from the behavior of ionization under ESI-MS conditions discussed before but confirming that the degree of dissociation of complex **Cu-2** in DCM solution is also the smallest. This least degree of dissociation also corresponds to the highest yield of complex **Cu-2** among the series.

Why $[Cu_2(BrphenBr)_2(dppb)_2]^{2+}$ is the most stable one among the series is worth exploring. According to the discussion of crystallography, both the larger P−Cu−P angles and the smaller dihedral angles contribute to the sterically close contact betweeen BrphenBr and diphosphine ligands and thus the stability to air and moisture in the solid state for complexes **Cu-1**−**Cu-4**. However, in DCM solutions, such close contact will cause a large repulsion between BrphenBr and diphosphine ligands and thus promote dissociation and ionization of cations. Because the dihedral angles between P−Cu−P and N−Cu−N planes in **Cu-1**−**Cu-4** are very close, the P−Cu−P angle becomes a very important factor for comparing the stability of cations in solutions. It is found that the P−Cu−P angle in complex **Cu-2**, 118.3(1)°, is the smallest, and such a relatively small angle will decrease the repulsion between diimine and diphosphine ligands. On the other hand, the conformation change of **Cu-2** is relatively simple compared with complexes **Cu-3** and **Cu-4**, which contain more $-CH_2$ groups. The above factors may be the reasons why $[Cu_2(BrphenBr)_2(dppb)_2]^{2+}$ is the most stable one among the series in solution.

It is worth mentioning that after being left in air for 4 months, no obvious change was observed for the corresponding absorption and emission spectra for solutions of **Cu-1**−**Cu-4** at 2.5×10^{-5} mol·L^{-1}, indicating that $[Cu_2(BrphenBr)_2(Ph_2P\text{-}(CH_2)_nPPh_2)_2]^{2+}$ ions are really stable from kinetics at some concentration range.

Photoluminescence (PL). The excitation and emission spectra of complexes **Cu-1**−**Cu-4** in the crystalline state were investigated at room temperature (see Figure 5), and the corresponding spectral data including emission wavelength, emission lifetimes, and solid-state photoluminescence quantum yield of complex **Cu-3** are listed in Table 1. Complexes **Cu-1**,

dx.doi.org/10.1021/ic402685u | Inorg. Chem. 2014, 53, 2922−2931

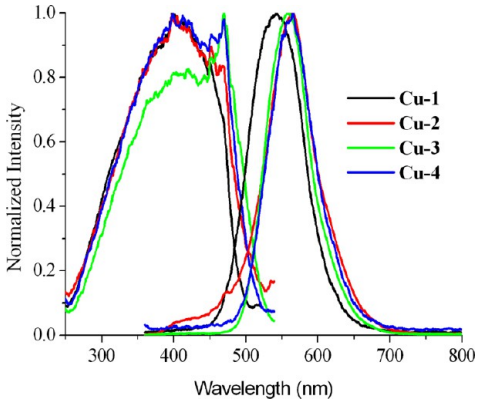

Figure 5. Excitation spectra (left) and emission spectra (right) with excitation wavelength at 330 nm of complexes **Cu-1**−**Cu-4** in the solid state at room temperature.

Cu-2, **Cu-3**, and **Cu-4** display intense emission bands with λ_{max} = 543, 565, 559, and 566 nm, respectively, which are assigned to a dπ(Cu) → π^*(diimine) (^{3}MLCT) excited state.[50,66−70] The emissive lifetimes, 2.51−9.26 μs, a little longer than those of $[Cu_2(BrbpyBr)_2(Ph_2P(CH_2)_nPPh_2)_2](ClO_4)_2$ complexes,[38] are perhaps related to the more rigid character of the BrphenBr ligand compared with BrbpyBr. The microsecond range lifetimes further confirm their triplet state character.

In order to get quantitative data and explore the factors affecting the luminescence, the emission quantum yield of complex **Cu-3** in the solid state were measured under air (see Table 1), because complex **Cu-3** in the solid state displayed the brightest emission under UV radiation of 365 nm. The emission quantum yield of complex **Cu-3**, 0.174, is 4.86 times that of mononuclear complex [Cu(BrphenBr)(bdpp)]-ClO_4·CH_2Cl_2[39] and very close to that of [Cu(phen)(bdpp)]-ClO_4·CH_2Cl_2, 0.1833, which has been suggested to arise from the triple $\pi\cdots\pi$ stacking interactions in the cation dimer and rich C−H$\cdots\pi$ interactions in the crystal structure.[39] Here, similar factors may also contribute to that of complex **Cu-3** because of the possible intermolecular $\pi\cdots\pi$ interaction, and the other possible factor may be the best protection of the Cu(I) centers by the close contact of BrphenBr and dpppen as discussed in the crystallographic part.

In DCM solutions with concentrations at 2.5 × 10^{-5} mol·L^{-1}, the emissions are too weak to be observed under radiation at 365 nm in air for complexes **Cu-1**−**Cu-4**. Only when the excitation and emission slits were wide enough to be 10 and 20 nm, respectively, could the emission curves be observed clearly (see Figure S29, Supporting Information). The emission bands before 490 nm probably arise from the intramolecular ligand-to-ligand charge transfer (^{1}LLCT) emission arising from the close contact of BrphenBr and diphosphine ligands in the complexes,[39] while the low-energy emission bands with maximum emission wavelengths from 561 to 572 nm are assigned to the ^{3}MLCT excited state, similar to those of solid emission.

Aggregation-Induced Phosphorescent Emission. On the basis of the very weak emissive characteristics in solution and intense phosphorescent behavior in the solid state along with the flexible $P(CH_2)_nP$ chains, complexes **Cu-1**−**Cu-4** are expected to show AIPE behavior. In order to investigate their AIPE attributes, different amounts of hexane, a poor solvent for complexes **Cu-1**−**Cu-4**, was added to the pure DCM solutions by defining the hexane fractions (f_h) of 0−90% and keeping the concentrations constant at 2.5 × 10^{-5} mol·L^{-1}. Figure 6 shows

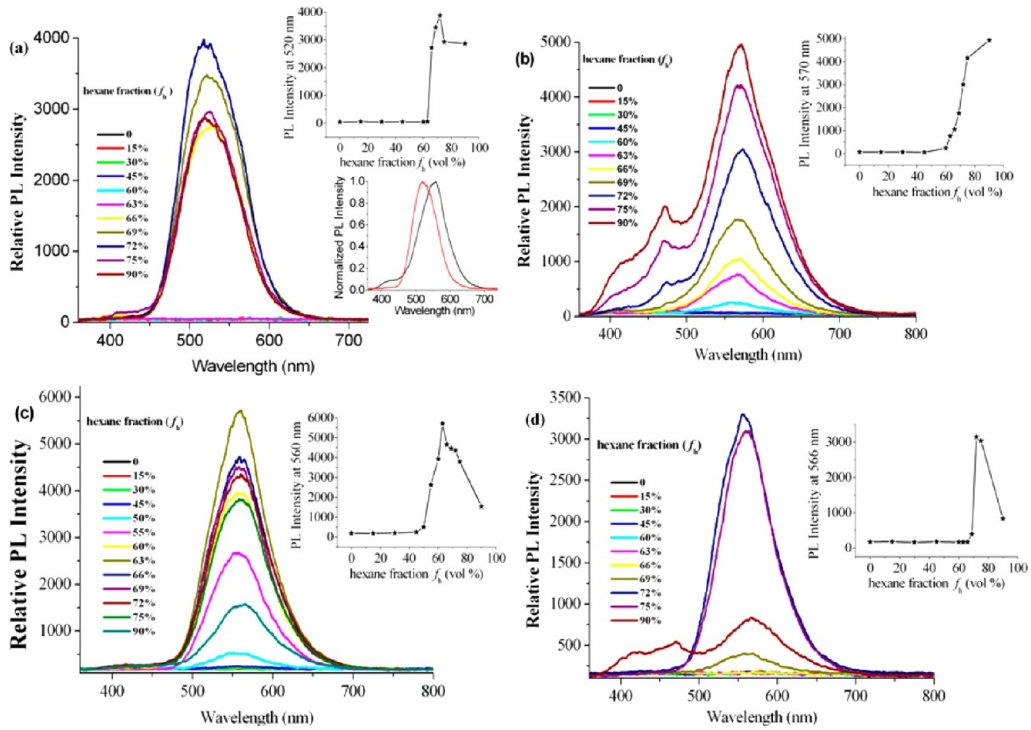

Figure 6. PL spectra of **Cu-1**−**Cu-4** in DCM/hexane mixed solvents with different f_h with excitation at 330 nm. (a) Insets depict the changes of PL peak intensity with different f_h (up) and the emission spectra at f_h = 90% of the freshly prepared one (black curve) and the one after 24 h of standing and 2 min ultrasonic reaction (red curve) (down); (b−d) insets depict the changes of PL peak intensity with different f_h. Excitation and emission slits are 2.5 and 2.5 nm for **Cu-1**, 5 and 5 nm for **Cu-2**, 2.5 and 2.5 nm for **Cu-3**, and 5 and 2.5 nm for **Cu-4**, respectively.

dx.doi.org/10.1021/ic402685u | Inorg. Chem. 2014, 53, 2922−2931

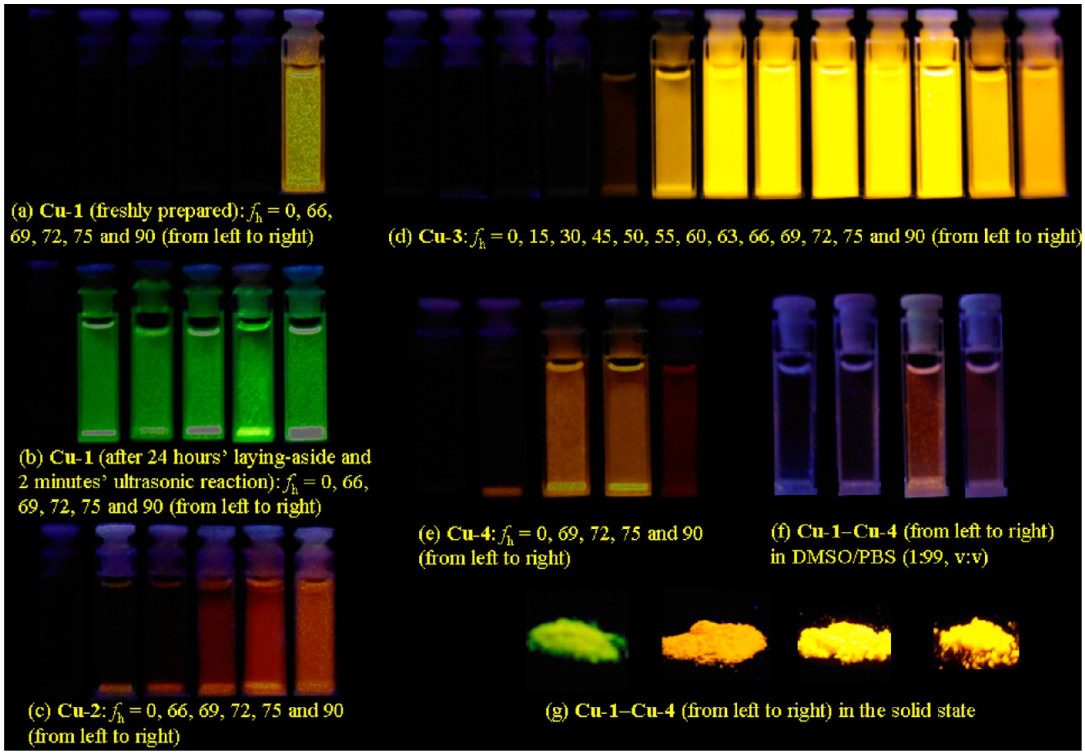

Figure 7. Luminescent images of **Cu-1**–**Cu-4** radiated with an ultraviolet light at 365 nm. (a–e) in hexane–DCM mixed solvents with the concentration kept at 2.5×10^{-5} mol·L^{-1}; (f) in DMSO/PBS (1:99, v:v) with concentration at 1.0×10^{-5} mol·L^{-1}; (g) in the solid state.

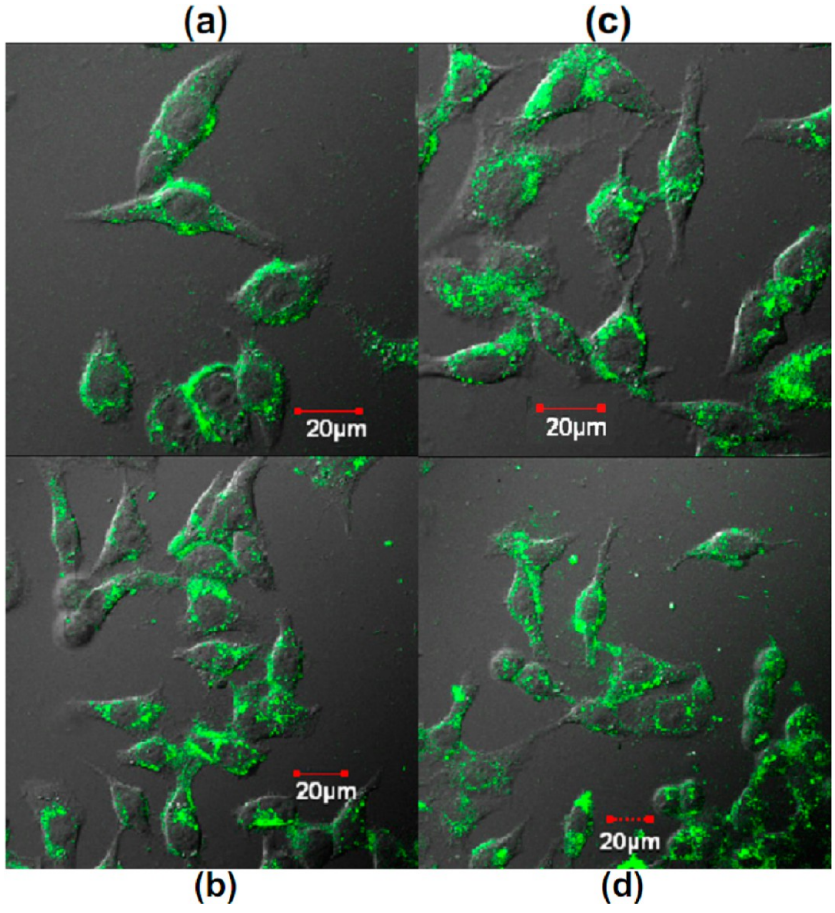

Figure 8. Confocal luminescence imaging of complexes **Cu-1**–**Cu-4** in HeLa cells, which were incubated with 10 μM complexes **Cu-1**–**Cu-4** in DMSO/PBS (1:99, v/v) for 15 min ((a) **Cu-1**, (b) **Cu-2**, (c) **Cu-3**, and (d) **Cu-4**).

dx.doi.org/10.1021/ic402685u | *Inorg. Chem.* 2014, 53, 2922–2931

the change of AIPE intensity of complexes **Cu-1**−**Cu-4** for different f_h with an excitation wavelength at 330 nm, which was selected with the comprehensive concern of the excitation maxima of the systems with f_h = 0, 90% for **Cu-1**, **Cu-3**, and **Cu-4** or f_h = 0, 75% for **Cu-2**, the excitation maxima of the systems with the brightest emission and necessary to obtain complete spectra (see Figure S30, Supporting Information). The luminescent images of **Cu-1**−**Cu-4** with different f_h and in the solid state under 365 nm radiation are shown in Figure 7. As shown in Figure 6, each of the complexes **Cu-1**, **Cu-2**, **Cu-3**, and **Cu-4** exhibits good AIPE behavior with the most intense emission appearing at f_h = 72%, 90%, 63%, and 72%, respectively. Complexes **Cu-1**−**Cu-4** exhibit various AIPE colors changing from yellow-green to orange-red. It is worth mentioning that for the freshly prepared systems, the AIPE phenomenon of **Cu-1** was not observed until f_h got to 90%, which was found to form the amorphous flocculent precipitate and show yellow emission. After 24 h of standing and then 2 min ultrasonically promoted reaction, the glittering laminar crystals were formed in the original supersaturated solutions with f_h in the range of 66−75%, and the amorphous flocculent precipitate for the system with f_h = 90% also changed to the glittering laminar crystals, which exhibit bright yellow-green emission with the maximum emission at about 520 nm, contrasting markedly with the nonemissive and yellow emissive behavior with the maximum emission at 558 nm for the corresponding freshly prepared ones (see Figures 6a, inset (down), and 7). The above phenomenon shows us that AIPE colors depend on the different aggregation states dramatically for complex **Cu-1.** Here, the restriction of intramolecular rotation was proposed to be responsible for the AIPE behavior of complexes **Cu-1**−**Cu-4**.

Bioimaging. Adding PBS solution to solutions of complexes **Cu-1**−**Cu-4** in DMSO leading to formation of amorphous flocculent precipitate and the corresponding AIE spectra of complexes **Cu-1**−**Cu-4** with a concentration of 10 μM in PBS/DMSO (99:1, v/v), similar to those of DCM solutions, are provided in Figure S31 (see Supporting Information). Luminescence imaging of complexes **Cu-1**−**Cu-4** in living HeLa cells was investigated through confocal luminescence microscopy with excitation at 405 nm. Incubation of HeLa cells with 10 μM complexes **Cu-1**−**Cu-4** in PBS/DMSO (99:1, v/v) for 15 min at 37 °C gave green intracellular luminescence imaging (Figure 8), among which imaging of complex **Cu-3** is the brightest. Because of the poor solubility and dispersity, it is difficult for complexes **Cu-1**−**Cu-4** to permeate into the cells completely, but to the best of our knowledge, this is the first time that aggregation-induced phosphorescence emissive Cu(I) complexes have been used for bioimaging. The green intracellular luminescence images contrast markedly with those red images in PBS/DMSO (99:1), and such a large difference is suggested to arise from the luminescence of intracellular background, the different states of aggregation in different environment, and the collected emission bands.

SUMMARY

A series of binuclear mixed-ligand copper(I) complexes, $[Cu_2(BrphenBr)_2(Ph_2P(CH_2)_nPPh_2)_2](ClO_4)_2$, ($n$ = 1, 4, 5, 6), was synthesized and characterized. The reasons why complexes **Cu-1**−**Cu-4** are very stable to air and moisture in the solid state are analyzed. The ESI-MS result through changing the collision cell energy from 0 to 20 eV suggests that the corresponding $[Cu_2(Ph_2P(CH_2)_nPPh_2)_2]^{2+}$ cations are the thermodynamically stable products and $[Cu_2(BrphenBr)_2(Ph_2P(CH_2)_nPPh_2)_2]^{2+}$ ions are stable products in crystallization kinetics in DCM solution. Both the results of ESI-MS and the dissociation behavior in DCM solution suggest that complex **Cu-2** is the most stable one among the series. Each of the complexes **Cu-1**−**Cu-4** displays good AIPE behavior and is used for living cell imaging successfully.

ASSOCIATED CONTENT

Supporting Information

Tables and figures giving additional photophysical results and X-ray crystallographic files in CIF format for determination of the four structures. This material is available free of charge via the Internet at http://pubs.acs.org. CCDC 951446, 951447, 960642, and 951448 contain supplementary crystallographic data for **Cu-1**·$2CH_2Cl_2$, **Cu-2**·$4CH_2Cl_2$, **Cu-3**·$2CH_3CN$, and **Cu-4**·$4CH_2Cl_2$. These data can be obtained free of charge via http://www.ccdc.cam.ac.uk/conts/retrieving.html or from the Cambridge Crystallographic Data Centre, 12 Union Road, Cambridge CB2 1EZ, UK. Fax: (+44) 1223-336-033. E-mail: deposit@ccdc.cam.ac.uk.

AUTHOR INFORMATION

Corresponding Authors

*E-mail: lxl@jsnu.edu.cn.
*E-mail: fyli@fudan.edu.cn.

Notes

The authors declare no competing financial interest.

ACKNOWLEDGMENTS

This work was supported financially by the National Natural Science Foundation of China (NSFC) (91027004, 21231004, 21375024, and 21271091), the Major Basic Research Project of Natural Science Foundation of the Jiangsu Higher Education Institutions (11KJA430009), and PAPD of Jiangsu Higher Education Institutions.

REFERENCES

(1) Chi, Y.; Chou, P. T. *Chem. Soc. Rev.* **2010**, *39*, 638.
(2) Zhao, Q.; Li, F.; Huang, C. *Chem. Soc. Rev.* **2010**, *39*, 3007.
(3) Lo, K. K. W.; Choi, A. W. T.; Law, W. H. T. *Dalton Trans.* **2012**, *41*, 6021.
(4) You, Y.; Nam, W. *Chem. Soc. Rev.* **2012**, *41*, 7061.
(5) Zhao, Q.; Huang, C.; Li, F. *Chem. Soc. Rev.* **2011**, *40*, 2508.
(6) Liu, L.; Li, X.; Hou, S.; Xue, Y.; Yao, Y.; Ma, Y.; Feng, X.; He, S.; Lu, Y.; Wang, Y.; Zeng, X. *Chem. Commun.* **2009**, 6759.
(7) Liu, Q.; Peng, J.; Sun, L.; Li, F. *ACS Nano* **2011**, *5*, 8040.
(8) Yang, T.; Xia, A.; Liu, Q.; Shi, M.; Wu, H.; Xiong, L.; Huang, C.; Li, F. *J. Mater. Chem.* **2011**, *21*, 5360.
(9) Sun, H.; Yang, L.; Yang, H.; Liu, S.; Xu, W.; Liu, X.; Tu, Z.; Su, H.; Zhao, Q.; Huang, W. *RSC Adv.* **2013**, *3*, 8766.
(10) Shi, H.; Sun, H.; Yang, H.; Liu, S.; Jenkins, G.; Feng, W.; Li, F.; Zhao, Q.; Liu, B.; Huang, W. *Adv. Funct. Mater.* **2013**, *23*, 3268.
(11) Liu, S.; Qiao, W.; Cao, G.; Chen, Y.; Ma, Y.; Huang, Y.; Liu, X.; Xu, W.; Zhao, Q.; Huang, W. *Macromol. Rapid Commun.* **2013**, *34*, 81.
(12) Lo, K. K. W.; Law, W. H. T.; Chan, J. C. Y.; Liu, H. W.; Zhang, K. Y. *Metallomics* **2013**, *5*, 808.
(13) Lo, K. K. W.; Chan, B. T. N.; Liu, H. W.; Zhang, K. Y.; Li, S. P. Y.; Tang, T. S. M. *Chem. Commun.* **2013**, *49*, 4271.
(14) Liu, J.; Liu, Y.; Liu, Q.; Li, C.; Sun, L.; Li, F. *J. Am. Chem. Soc.* **2011**, *133*, 15276.

(15) Ma, Y.; Liu, S.; Yang, H.; Wu, Y.; Yang, C.; Liu, X.; Zhao, Q.; Wu, H.; Liang, J.; Li, Y.; Huang, W. *J. Mater. Chem.* **2011**, *21*, 18974.
(16) Lo, K. K. W.; Li, S. P. Y.; Zhang, K. Y. *New J. Chem.* **2011**, *35*, 265.
(17) Liu, S.; Sun, H.; Ma, Y.; Ye, S.; Liu, X.; Zhou, X.; Mou, X.; Wang, L.; Zhao, Q.; Huang, W. *J. Mater. Chem.* **2012**, *22*, 22167.
(18) Mou, X.; Wu, Y.; Liu, S.; Shi, M.; Liu, X.; Wang, C.; Sun, S.; Zhao, Q.; Zhou, X.; Huang, W. *J. Mater. Chem.* **2011**, *21*, 13951.
(19) Yang, Y.; Zhao, Q.; Feng, W.; Li, F. *Chem. Rev.* **2013**, *113*, 192.
(20) Chen, X. L.; Yu, R.; Zhang, Q. K.; Zhou, L. J.; Wu, X. Y.; Zhang, Q.; Lu, C. Z. *Chem. Mater.* **2013**, *25*, 3910.
(21) Volz, D.; Zink, D. M.; Bocksrocker, T.; Friedrichs, J.; Nieger, M.; Baumann, T.; Lemmer, U.; Braese, S. *Chem. Mater.* **2013**, *25*, 3414.
(22) Czerwieniec, R.; Kowalski, K.; Yersin, H. *Dalton Trans.* **2013**, *42*, 9826.
(23) Zink, D. M.; Bäechle, M.; Baumann, T.; Nieger, M.; Kühn, M.; Wang, C.; Klopper, W.; Monkowius, U.; Hofbeck, T.; Yersin, H.; Bräse, S. *Inorg. Chem.* **2013**, *52*, 2292.
(24) Zhang, Q.; Komino, T.; Huang, S.; Matsunami, S.; Goushi, K.; Adachi, C. *Adv. Funct. Mater.* **2012**, *22*, 2327.
(25) Czerwieniec, R.; Yu, J. B; Yersin, H. *Inorg. Chem.* **2011**, *50*, 8293.
(26) Hsu, C. W.; Lin, C. C.; Chung, M. W.; Chi, Y.; Lee, G. H.; Chou, P. T.; Chang, C. H.; Chen, P. Y. *J. Am. Chem. Soc.* **2011**, *133*, 12085.
(27) Hashimoto, M.; Igawa, S.; Yashima, M.; Kawata, I.; Hoshino, M.; Osawa, M. J. *Am. Chem. Soc.* **2011**, *133*, 10348.
(28) Liu, Z.; Qayyum, M. F.; Wu, C.; Whited, M. T.; Djurovich, P. I.; Hodgson, K. O.; Hedman, B.; Solomon, E. I.; Thompson, M. E. *J. Am. Chem. Soc.* **2011**, *133*, 3700.
(29) Min, J.; Zhang, Q.; Sun, W.; Cheng, Y.; Wang, L. *Dalton Trans.* **2011**, *40*, 686.
(30) Deaton, J. C.; Switalski, S. C.; Kondakov, D. Y.; Young, R. H.; Pawlik, T. D.; Giesen, D. J.; Harkins, S. B.; Miller, A. J. M.; Mickenberg, S. F.; Peters, J. C. *J. Am. Chem. Soc.* **2010**, *132*, 9499.
(31) Luo, S. P.; Mejía, E.; Friedrich, A.; Pazidis, A.; Junge, H.; Surkus, A.; Jackstell, R.; Denurra, S.; Gladiali, S.; Lochbrunner, S.; Beller, M. *Angew. Chem., Int. Ed.* **2013**, *52*, 419.
(32) Linfoot, C. L.; Richardson, P.; Hewat, T. E.; Moudam, O.; Forde, M. M.; Collins, A.; White, F.; Robertson, N. *Dalton Trans.* **2010**, 8945.
(33) Xu, X. Y.; Xiao, H. N.; Xu, Y. M.; Zhang, M. J. *Spectrochim. Acta, A* **2012**, *95*, 427.
(34) Zhou, C.; Wang, Q. *Transition Met. Chem.* **2010**, *35*, 605.
(35) Li, Z. *Spectrochim. Acta, A* **2011**, *81*, 475.
(36) Wen, C.; Tao, G.; Xu, X.; Feng, X.; Luo, R. *Spectrochim. Acta, A* **2011**, *79*, 1345.
(37) Smith, C. S.; Branham, C. W.; Marquard, B. J.; Mann, K. R. *J. Am. Chem. Soc.* **2010**, *132*, 14079.
(38) Li, X. L.; Xin, X. L.; Ai, Y. B.; Tan, M.; Lu, H.; Du, B. X. *Inorg. Chim. Acta* **2013**, *401*, 58.
(39) Li, X. L.; Ai, Y. B.; Yang, B.; Chen, J.; Tan, M.; Xin, X. L.; Shi, Y. S. *Polyhedron* **2012**, *35*, 47.
(40) Suh, H.; Casadonte, D. J., Jr.; Hope-Weeks, L.; Kim, H.; Kim, B.; Chang, T. *Inorg. Chim. Acta* **2013**, *394*, 710.
(41) Horvath, R.; Fraser, M. G.; Cameron, S. A.; Blackman, A. G.; Wagner, P.; Officer, D. L.; Gordon, K. C. *Inorg. Chem.* **2013**, *52*, 1304.
(42) Fazal, A.; Ali, B. E.; Ouahab, L.; Fettouhi, M. *Polyhedron* **2013**, *49*, 7.
(43) Andrés-Tomé, I.; Fyson, J.; Baiao Dias, F.; Monkman, A. P.; Iacobellis, G.; Coppo, P. *Dalton Trans.* **2012**, *41*, 8669.
(44) Zhang, L.; Yue, S.; Li, B.; Fan, D. *Inorg. Chim. Acta* **2012**, *384*, 225.
(45) Smirnova, E. S.; Melekhova, A. A.; Gurzhiy, V. V.; Selivanov, S. I.; Krupenya, D. V.; Koshevoy, I. O.; Tunik, S. P. *Z. Anorg. Allg. Chem.* **2012**, *638*, 415.
(46) Costa, R. D.; Tordera, D.; Qrti, E.; Bolink, H. J.; Schönle, J.; Graber, S.; Housecroft, C. E.; Constable, E. C.; Zampese, J. A. *J. Mater. Chem.* **2011**, *21*, 16108.
(47) Hou, R.; Huang, T.; Wang, X.; Jiang, X.; Ni, Q.; Gui, L.; Fan, Y.; Tan, Y. *Dalton Trans.* **2011**, 7551.
(48) Vorontsov, I. I.; Andrey, T. G.; Kovalevsky, Y.; Novozhilova, I. V.; Gembicky, M.; Chen, Y. S.; Coppens, P. *J. Am. Chem. Soc.* **2009**, *131*, 6566.
(49) Zhang, L.; Li, B.; Su, Z. *Langmuir* **2009**, *25*, 2068.
(50) Shi, L.; Li, B. *Eur. J. Inorg. Chem.* **2009**, *48*, 2294.
(51) Zhang, Q.; Ding, J.; Cheng, Y.; Wang, L.; Xie, Z.; Jing, X.; Wang, F. *Adv. Funct. Mater.* **2007**, *17*, 2983.
(52) Cuttell, D. G.; Kuang, S.; Fanwick, P. E.; McMillin, D. R.; Walton, R. A. *J. Am. Chem. Soc.* **2002**, *124*, 6.
(53) Saito, K.; Arai, T.; Takahashi, N.; Tsukuda, T.; Tsubomura, T. *Dalton Trans.* **2006**, 4444.
(54) Coppens, P. *Chem. Commun.* **2003**, 1317.
(55) Coppens, P.; Vorontsov, I. I.; Graber, T.; Kovalevsky, A. Y.; Chen, Y. S.; Wu, G.; Gembicky, M.; Novozhilova, I. V. *J. Am. Chem. Soc.* **2004**, *126*, 5980.
(56) Tzalis, D.; Tor, Y.; Failla, S.; Siegel, J. S. *Tetrahedron Lett.* **1995**, *36*, 3489.
(57) Dietrich-Buchecker, C.; Sauvage, J. P.; Kern, J. M. *J. Am. Chem. Soc.* **1989**, *111*, 7791.
(58) Wrighton, M. S.; Ginley, D. S.; Morse, D. L. *J. Phys. Chem.* **1974**, *78*, 2229.
(59) Rigaku. *CrystalClear*; Rigaku Corporation: Tokyo, Japan, 2005.
(60) Bruker. *SAINT*; Bruker AXS Inc.; Madison, WI, USA, 2001.
(61) Rigaku. *CrystalClear*; Rigaku Corp.: Tokyo, Japan, 2007.
(62) Sheldrick, G. M. *SHELXL-97, Program for the Refinement of Crystal Structures*; University of Göttingen: Göttingen, Germany, 1997.
(63) Pearson, R. G. *J. Am. Chem. Soc.* **1963**, *85*, 3533.
(64) Armaroli, N.; Accorsi, G.; Bergamini, G.; Ceroni, P.; Holler, M.; Moudam, O.; Duhayon, C.; Delavaux-Nicot, B.; Nierengarten, J. F. *Inorg. Chim. Acta* **2007**, *360*, 1032.
(65) Wang, Z.; Cao, Q.; Huang, X.; Lin, S.; Gao, X. *Inorg. Chim. Acta* **2010**, *363*, 15.
(66) Moudam, O.; Kaeser, A.; Delavaux-Nicot, B.; Duhayon, C.; Holler, M.; Accorsi, G.; Armaroli, N.; Séguy, I.; Navarro, J.; Destruel, P.; Nierengarten, J. *Chem. Commun.* **2007**, 3077.
(67) Kuang, S. M.; Cuttell, D. G.; McMillin, D. R.; Fanwick, P. E.; Walton, R. A. *Inorg. Chem.* **2002**, *41*, 3313.
(68) Listorti, A.; Accorsi, G.; Rio, Y.; Armaroli, N.; Moudam, O.; Gégout, A.; Delavaux-Nicot, B.; Holler, M.; Nierengarten, J. *Inorg. Chem.* **2008**, *47*, 6254.
(69) Zhang, L.; Li, B. *Inorg. Chim. Acta* **2009**, *362*, 4857.
(70) Si, Z.; Li, J.; Li, B.; Liu, S.; Li, W. *J. Lumin.* **2008**, *128*, 1303.